Scatchard, G. (1949) *Ann. N.Y. Acad. Sci. 51*, 660–672.
Scharf, S. J., Horn, G. T., & Erlich, H. A. (1986) *Science 233*, 1076–1078.
Scheel, J., Ziegelbauer, K., Kupke, T., Humbel, B., Noegel, A. A., Gerisch, G., & Schleicher, M. (1989) *J. Biol. Chem. 264*, 2832–2839.
Schleicher, M., Andrē, E., Hartmann, H., & Noegel, A. A. (1988) *Dev. Genet. (N.Y.) 9*, 521–530.
Simon, M.-N., Mutzel, R., Mutzel, H., & Veron, M. (1988) *Plasmid 19*, 94–102.
Spudich, J. A., & Watt, S. (1971) *J. Biol. Chem. 246*, 4866–4871.
Stossel, T. P. (1989) *J. Biol. Chem. 264*, 18261–18264.
Stossel, T. P., Chaponnier, C., Ezzell, R. M., Hartwig, J. H., Janmey, P. A., Kwiatkowski, D. J., Lind, S. E., Smith, D. B., Southwick, F. S., Yin, H. L., & Zaner, K. S. (1985) *Annu. Rev. Cell Biol. 1*, 353–402.
Vandekerckhove, J. (1990) *Curr. Opin. Cell Biol. 2*, 41–50.
Walsh, T. P., Weber, A., Davis, K., Bonder, E., & Mooseker, M. (1984) *Biochemistry 23*, 6099–6102.
Way, M., & Weeds, A. (1988) *J. Mol. Biol. 203*, 1127–1133.
Yin, H. L., & Stossel, T. P. (1979) *Nature 281*, 581–586.
Yin, H. L., Janmey, P. A., & Schleicher, M. (1990) *FEBS Lett. 264*, 78–80.

Inhibition of Myosin ATPase by Beryllium Fluoride†

Brigitte Phan and Emil Reisler*
Department of Chemistry and Biochemistry and Molecular Biology Institute, University of California, Los Angeles, California 90024

Received November 1, 1991; Revised Manuscript Received March 13, 1992

ABSTRACT: Inhibition of the myosin subfragment 1 (S-1) ATPase activity by beryllium fluoride was studied directly in the presence of MgATP and following preincubation of samples with MgADP. In both cases, the rates of inhibition were very slow, with k_{app} = 0.5 and 58 M^{-1} s^{-1}, respectively, in analogy to the rates of inhibition of myosin ATPase by vanadate [Goodno, C. C. (1979) *Proc. Natl. Acad. Sci. U.S.A. 76*, 2620–2624]. The very different rates of inhibition in the presence of MgATP and on preincubation with MgADP suggested that beryllium fluoride binds to the M·ADP state of myosin. The slow inhibition rates and the nonlinear dependence of the observed rates on beryllium fluoride concentration were consistent with a two-step inhibition process involving a rapid binding equilibrium to yield a collisional complex, M·ADP·BeF_3^-, and its slow isomerization into M*·ADP·BeF_3^-. A third, much slower, step was required to account for the conversion of the stable M*·ADP·BeF_3^- to a virtually irreversibly inhibited complex. Kinetic description of the inhibition pathway was derived from the observed rates of inhibition of myosin ATPase, information on the binding of beryllium fluoride to M·ADP, and measurements of ϵADP chase from M*·ϵADP·BeF_3^-. The isomerization rate and equilibrium constants were 1.4×10^{-2} s^{-1} and 50, respectively, and the overall binding constant of beryllium fluoride to M·ADP was 5×10^5 M^{-1}. The inhibitory complex showed a 16% enhancement to tryptophan fluorescence of S-1 and a reduced quenching of ϵADP by acrylamide. It is concluded that M*·ADP·BeF_3^- is analogous to the M*·ADP·V_i and M**·ADP·P_i states of myosin.

Muscles produce force by cyclic interactions between filaments of actin and myosin which are coupled to the hydrolysis of ATP. The simplified four-step scheme for myosin-catalyzed hydrolysis of ATP in the presence of Mg^{2+}, according to Bagshaw and Trentham (1973), is depicted in Scheme I where M, M*·ATP, M**·ADP·P_i, and M*·ADP represent conformational states of myosin–nucleotide complexes having distinct spectral properties. At room temperature, the predominant steady-state intermediate is the species M**·ADP·P_i. This transition state is believed to be a key intermediate in the energy transduction process (Johnson & Taylor, 1978). Thus, there is considerable interest in the characterization of the M**·ADP·P_i state and in developing appropriate probes for that purpose.

Scheme I

$$M + ATP \leftrightarrow M^*\cdot ATP \leftrightarrow M^{**}\cdot ADP\cdot P_i \leftrightarrow M^*\cdot ADP \leftrightarrow M + ADP$$

Vanadate, a well-known inorganic phosphate analogue [for a review, see Goodno (1982)], has been used extensively to characterize the M**·ADP·P_i state. In the presence of ADP, vanadate binds to the active site of myosin and forms an inactive ternary complex, M*·ADP·V_i. As suggested by X-ray diffraction studies with glycerinated muscle (Goody et al., 1980) and spin-label experiments (Wells & Bagshaw, 1984), this complex is conformationally analogous to the intermediate M**·ADP·P_i species. However, the tendency of vanadate to polymerize and its absorption in the UV region significantly limit its use. Therefore, additional phosphate analogues would facilitate further characterization of the M**·ADP·P_i state of myosin.

The complexes of aluminum and beryllium with fluoride, AlF_4^- and BeF_3^-, belong to a relatively new class of phosphate analogues which affect the activities of several G proteins (Bigay et al., 1987), phosphatases (Lange et al., 1986), and ATPases (Robinson et al., 1986). Recently, AlF_4^- and BeF_3^- were shown to bind to the catalytic sites of the beef F_1-ATPase with a stoichiometry of one metal per catalytic site and to inhibit the F_1-ATPase (Issartel et al., 1991). The essentially

† This work was supported by Grant AR22031 and Atherosclerosis Training Grant HL 07386 from the National Institutes of Health and by Grant DMB 89-05363 from the National Science Foundation.

0006-2960/92/0431-4787$03.00/0

irreversible inhibition of F_1-ATPase was correlated with the tight binding of fluorometal to F1 (Issartel et al., 1991). AlF_4^- and BeF_3^- have also been used as phosphate analogues to probe the mechanism of ATP hydrolysis by F-actin (Combeau & Carlier, 1988). These compounds stabilized F-ADP–actin in a phosphate-like fashion; i.e., they bound to F-ADP–actin with a strong affinity in competition with inorganic phosphate, and dissociated from F-ADP–actin very slowly ($k_{off} = 8 \times 10^{-6}$ s^{-1}). Closer to myosin, the most recent study of Chase and Kushmerick (1991) showed that aluminum fluoride was a potent inhibitor of force generation in skinned muscle fibers. Furthermore, the aluminum and beryllium fluoride complexes were also found to inhibit the MgATPase activity of both smooth and skeletal heavy meromyosin, by forming stable, ternary complexes of myosin·ADP·BeF_3^- and myosin·ADP·AlF_4^- (Maruta et al., 1991).

The goal of the present study was to characterize the interactions of beryllium fluoride with myosin. We show that in the presence of ADP, BeF_3^- binds strongly to the active site of myosin, and the resulting inactive ternary complex, denoted M^*·ADP·BeF_3^-, adopts a conformation similar to that of the intermediate M^{**}·ADP·P_i state.

Materials and Methods

Reagents. ADP, ATP, Be, and NaF were purchased from Sigma Chemical Co. (St. Louis, MO). 1,N^6-Ethenoadenosine diphosphate (ϵADP)[1] was obtained from Molecular Probes Inc. (Junction City, OR). Crystalline acrylamide was obtained from Bio-Rad (Richmond, CA). Millipore-filtered distilled water and analytical-grade reagents were used in all experiments. Note that Be is toxic and may be carcinogenic, and should be handled carefully.

Proteins. Myosin from rabbit psoas muscle was prepared according to Godfrey and Harrington (1970). Subfragment 1 (S-1) was prepared by chymotryptic digestion of myosin as described by Weeds and Pope (1977). S-1 was not separated into isozymes and was used as a mixture of S-1 (A1) and S-1 (A2). Its concentration was determined spectrophotometrically by using $E^{1\%}_{280nm} = 7.5$ cm^{-1} (Wagner & Weeds, 1977).

ATPase Assays. K^+(EDTA) ATPase assays were performed according to the method of Kielly and Bradley (1956). Colorimetric MgATPase assays were carried out in 40 mM KCl, 2 mM $MgCl_2$, and 10 mM Tris-HCl, pH 7.6 (solvent A), at 25 °C by the addition of 1 mM MgATP to 3 μM S-1. The reaction was stopped with 10% trichloroacetic acid.

Effects of Be and NaF on ATPase Activities of S-1. These effects were monitored by measuring the percentage inhibition of ATPase activity of S-1. The inhibition of activity was much more effective when S-1 (3 μM) was preincubated with ADP (300 μM), $MgCl_2$ (2 mM), Be (100 μM), and NaF (5 mM) prior to ATP addition.

The rate constants for changes in the ATPase activity of S-1 were calculated from the inhibition of MgATPase activity as a function of preincubation time with MgADP and BeF_3^-. Briefly, S-1 (3 μM) and ADP (300 μM), $MgCl_2$ (2 mM), Be (100 μM), and NaF (5 mM) were preincubated for various times (from 0 to 60 min). The ATPase activities at different preincubation times were expressed relative to the control ATPase activity (zero preincubation time). The rate constants for activity changes were determined from the initial slopes of semilogarithmic plots relating the percentage of S-1 ATPase activity and the preincubation time.

Binding of Beryllium Fluoride to S-1. The amount of beryllium fluoride bound to S-1 at any given Be concentration was obtained from the percentage inhibition of ATPase activity, assuming that at saturating Be concentrations, where the inhibition approached 100%, the molar ratio of BeF_3^-/S-1 bound = 1 (Maruta et al., 1991). Scatchard plots for the binding of beryllium fluoride to S-1 were constructed by expressing the amount of beryllium fluoride bound (derived from the percentage inhibition of MgATPase activity) as a function of beryllium concentration. The concentration of fluoride was set to its optimal value for full inhibition of S-1 ATPase activity.

Release of BeF_3^- from S-1. The release of the inhibitory complex from S-1 was monitored by measuring the ATPase activity of the inhibited S-1 as a function of dialysis time against solvent A. Briefly, S-1 (10 μM) was incubated with ADP (1 mM), Be (300 μM), and NaF (5 mM) in solvent A for 45 min at 25 °C. The reaction mixture was then dialyzed against 50 volumes of 40 mM KCl, 10 mM Tris-HCl, and 5 mM EDTA, pH 7.6 (changed twice daily). Aliquots of the dialyzed S-1 were taken at given times for K^+(EDTA) ATPase activity measurements. All recovered activities were expressed relative to those of the control sample (no Be and NaF) which was treated similarly.

Chase Experiments. Chase experiments were carried out by measuring the fluorescence intensity of ϵADP in the presence of a quencher, acrylamide, which preferentially quenches free ϵADP (Ando et al., 1982). Thus, the presence of acrylamide in solution amplifies the spectral difference between bound and free ϵADP. Briefly, S-1 (18 μM) was preincubated with ϵADP (15 μM) in the presence or absence of beryllium fluoride for 10 min at 25 °C unless specified otherwise. The standard solvent contained 10 mM PIPES, 30 mM KCl, and 1 mM $MgCl_2$, pH 7.0. The fluorescence of ϵADP was measured in the presence of 100 mM acrylamide. The chase of ϵADP bound to S-1 was carried out with ADP ranging in concentrations between 10 μM and 1.5 mM.

Fluorescence Measurements. The accessibility of ϵADP to collisional quenchers was examined by titrating ϵADP with acrylamide in the presence and absence of BeF_3^-. Briefly, S-1 with a substoichiometric amount of ϵADP (0.3 ϵADP/S-1), with or without BeF_3^-, was placed in a cuvette, and the fluorescence emission was measured as a function of increasing acrylamide concentrations (Ando et al., 1978). Stern–Volmer plots were prepared according to Lehrer and Leavis (1978).

All fluorescence measurements for ϵADP were conducted at 25 °C in a Spex Fluorolog spectrophotometer (Spex Industries, Inc., Edison, NJ) at excitation and emission wavelengths of 330 and 410 nm, respectively.

Tryptophan fluorescence was also measured at 25 °C in the Spex Fluorolog spectrophotometer, at excitation and emission wavelengths of 295 and 340 nm, respectively (Werber et al., 1972). The tryptophan fluorescence of S-1 (15 μM) in solvent A was measured first; then following the additions of ATP (0.1 mM), ADP (0.1 mM), and ADP (0.1 mM) + Be (0.1 mM) + NaF (5 mM), the fluorescence of S-1 was measured again. All fluorescence intensities were corrected for dilution effects and normalized to the intensity of S-1 alone.

Results

BeF_3^- Inhibits the ATPase Activity of S-1. The complexes of aluminum and beryllium with fluoride have been shown to inhibit the mitochondrial F_1-ATPase (Issartel et al., 1991) and the smooth muscle myosin ATPase (Maruta et al., 1991). To verify that BeF_3^- behaves as a phosphate analogue in our system, the effect of BeF_3^- on skeletal myosin ATPase was

[1] Abbreviations: S-1, myosin subfragment 1; ϵADP, 1,N^6-ethenoadenosine diphosphate; V_i, vanadate ion.

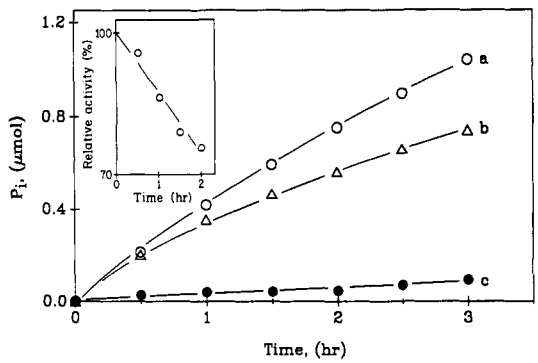

FIGURE 1: Inhibition of MgATPase activity of S-1 by BeF_3^-. Release of P_i as a function of time was measured in solutions containing solvent A, 3 μM S-1, and 1 mM ATP (in a total volume of 1.0 mL) at 25 °C. The concentrations of ADP, Be, and NaF when present were 300 μM, 100 μM, and 5 mM, respectively. Curve a (○) corresponds to control measurements, i.e., assays carried out in the absence of ADP, Be, and NaF. Curve b (△) represents MgATPase activities assayed in the presence of Be and NaF. Curve c (●) corresponds to measurements of MgATPase activities assayed in the presence of ADP, Be, and NaF which were preincubated with S-1 for 30 min prior to ATP addition. Inset: semilogarithmic plot of the residual ATPase activity (%) versus time. Each point corresponds to a ratio of the respective data points taken from curves b and a. The slope gives a value of $k_{obs} = 4.8 \times 10^{-5}$ s^{-1}.

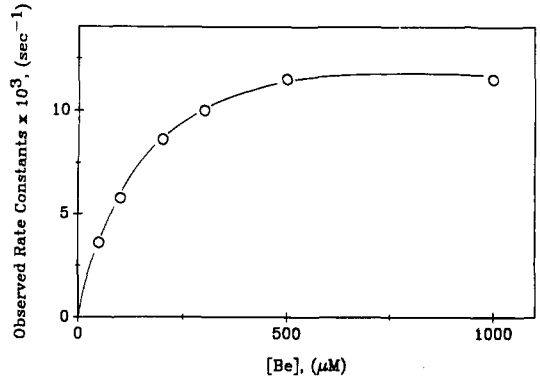

FIGURE 2: Rates of ATPase change as a function of Be concentration. The observed rates were obtained from semilogarithmic plots of ATPase activity as a function of preincubation time of S-1 with MgADP and BeF_3^-. Final concentrations of all components were as follows: S-1, 3 μM; ADP, 300 μM; NaF, 5 mM; Be, as indicated.

examined. As shown in Figure 1, BeF_3^- was an effective inhibitor of the skeletal myosin MgATPase. Beryllium alone did not have any effect on myosin activity while fluoride alone inhibited slightly the ATPase (up to 5%). The latter effect was produced most likely by the presence of trace amounts of Al^{3+} ions in buffers and nucleotide solutions. Without preincubation, the inhibition of S-1 ATPase by BeF_3^- was slow (Figure 1, curve b). The rate constant (k_{obs}) for the progressive inhibition of MgATPase activity of S-1, estimated from the semilogarithmic plot of the residual ATPase activity versus time (inset to Figure 1), was 4.8×10^{-5} s^{-1}, corresponding to an apparent second-order rate constant (k_{app}) of 0.48 M^{-1} s^{-1}. Very similar rates and slow onset of inhibition of ATPase activity were also observed for myosin and vanadate (Goodno, 1979).

More efficient and faster inhibition of S-1 MgATPase was obtained when BeF_3^- was preincubated with S-1 and MgADP prior to the addition of ATP (Figure 1, curve c). Similarly, Ca^{2+} and K^+(EDTA) ATPase activities of S-1 preincubated with ADP and BeF_3^- were inhibited strongly (data not shown). The inhibition of MgATPase activity of S-1 caused by its preincubation with MgADP, beryllium, and fluoride depended on the preincubation time. The observed rate of inactivation (k_{obs}) in the presence of 100 μM Be, determined from semilogarithmic plots of ATPase activity versus time of preincubation, was 5.8×10^{-3} s^{-1} (not shown), corresponding to an apparent second-order rate constant (k_{app}) of 58 M^{-1} s^{-1}. This result shows that the formation of the inhibitory complex is slow even in the presence of MgADP. In analogy to the mechanism postulated for vanadate inhibition of myosin ATPase activity (Goodno, 1979), this process most likely consists of relatively fast equilibrium binding followed by a slow isomerization step:

$$\text{M·ADP} + \text{Be} + \text{NaF} \underset{k_{-1}}{\overset{k_1}{\rightleftharpoons}} \text{M·ADP·BeF}_3^- \underset{k_{-2}}{\overset{k_2}{\rightleftharpoons}} \text{M}^*\text{·ADP·BeF}_3^- \quad (1)$$

To determine the maximum rate of inhibition of S-1 MgATPase by BeF_3^- and test the two-step inhibition mechanism, various concentrations of beryllium were mixed with M·ADP (with fluoride in excess), and the time course of ATPase activity changes was followed. The observed rate constants for activity changes were then plotted in Figure 2 as a function of beryllium concentration. The maximum rate of inhibition determined from Figure 2 was 1.15×10^{-2} s^{-1}. The observed rates did not increase linearly with beryllium concentration, excluding a one-step mechanism for BeF_3^- binding to M·ADP and consistent with the slow isomerization step limiting the rate of the entire process.

A customary analysis of the observed rate constants for a mechanism proposed in eq 1 can be carried out according to eq 2 [e.g., eq 4–47 in Fersht (1977)] where K_1 is the equi-

$$(k_{obs} - k_{-2})^{-1} = k_2^{-1} + (K_1 k_2 [\text{Be}])^{-1} \quad (2)$$

librium constant for the first step of the reaction, the formation of the collisional complex M·ADP·BeF_3^-. When the data of Figure 2 were replotted according to eq 2, a linear plot was obtained (not shown), consistent with the proposed mechanism. The values of k_2 and K_1 derived from the plot were 1.43×10^{-2} s^{-1} and 6.0×10^3 M^{-1}, respectively. The value of k_{-2} used in this calculation (4.0×10^{-4} s^{-1}) was the k_{off} taken from εADP chase experiments shown in Figure 5. The choice of this k_{-2} value is rationalized under Discussion.

Binding of Beryllium Fluoride to S-1 and Stability of the M·ADP·BeF_3^- Complex. Since the binding of BeF_3^- to S-1 inhibits its ATPase activity, the association constant of beryllium fluoride to M·ADP can be indirectly determined by measuring the percentage inhibition of the ATPase activity by BeF_3^-. This approach is based on the assumption that the inhibition of myosin ATPase is caused by the formation of a stoichiometric 1:1 complex of M·ADP and BeF_3^-. The above assumption is supported by the findings that aluminum and beryllium fluorides bind to the catalytic sites of beef F_1-ATPase (Issartel et al., 1991), actin·ADP (Combeau & Carlier, 1988), and heavy meromyosin (Maruta et al., 1991) with a stoichiometry of 1 to 1. Figure 3 shows the Scatchard plot for the binding of Be to S-1. The association constant determined from this plot was 5×10^5 M^{-1}. This value is higher than the association constant of vanadate to S-1 (Goodno, 1979; Wells & Bagshaw, 1984), indicating that beryllium fluoride binds to M·ADP with greater affinity. Similarly, beryllium fluoride has also been found to bind to F-ADP–actin with much higher affinity than vanadate (Combeau & Carlier, 1988).

The ternary complex formed between BeF_3^- and M·ADP is very stable. As shown in Figure 4, only between 20 and 25% of S-1 ATPase activity was recovered after extensive dialysis, much of it during the first 24 h. The slow and limited dissociation of the ternary complex M*·ADP·BeF_3^- resembles that

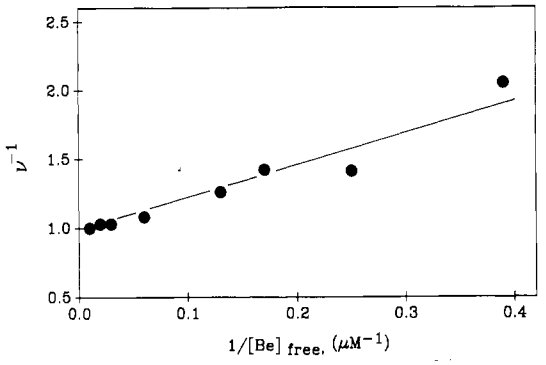

FIGURE 3: Scatchard plot for the binding of BeF_3^- to S-1. The binding of BeF_3^- to S-1 was monitored by measuring the inhibition of S-1 MgATPase activity by BeF_3^-. The amount of BeF_3^- bound to S-1 (3 μM) at any given Be concentration was derived from the percentage inhibition of S-1 ATPase activity by assuming that at saturating Be concentrations, at which the MgATPase inhibition approached 100%, the molar ratio of $BeF_3^-/S\text{-}1_{bound}$ was 1.0. ν corresponds to the ratio of S-1 with Be bound to it over total S-1. The MgATPase assays contained S-1 (3 μM), ADP (300 μM), $MgCl_2$ (2 mM), NaF (5 mM), and Be between 0 and 100 μM. All preincubations were for 45 min.

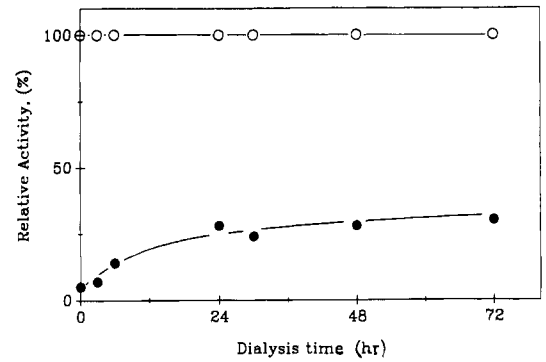

FIGURE 4: Dialysis of the M·ADP·BeF_3^- complex. The stability of the M·ADP·BeF_3^- complex was examined by measuring the recovery of the ATPase activity of the inhibited S-1 as a function of dialysis time. S-1 (10 μM) was inactivated by a 45-min incubation with 1 mM ADP, 300 μM Be, and 5 mM NaF in solvent A at 25 °C. The dialysis of the S-1·ADP·BeF_3^- complex was carried out at 4 °C against 50 volumes of solvent A in the presence of 5 mM EDTA (changed twice daily). The EDTA ATPase activity was measured on aliquots of the dialyzed S-1. Activities of the inhibited S-1 (●) were expressed relative to the activity of the control sample (○) which was treated similarly.

of the complex formed between myosin, ADP, and vanadate (Goodno, 1979). However, the stable inhibition was reversed completely by actin, along with nucleotide release (not shown), confirming the reversible nature of the M*·ADP·BeF_3^- complex. The inhibition of the beef F_1-ATPase by beryllium fluoride, on the other hand, was irreversible (Issartel et al., 1991). The irreversible inhibition has been attributed to the tight binding of BeF_3^- to F-1 (Issartel et al., 1991).

Release of ϵADP from S-1. The release of ϵADP from S-1 was examined by chasing the bound ϵADP with ADP and monitoring the resulting time-dependent changes in fluorescence. The rationale for these experiments relied on the preferential quenching of free ϵADP by acrylamide (Ando et al., 1982). The fluorescent signal of ϵADP bound to myosin is high, but when the analogue is displaced from S-1 by ADP and released into the medium, its fluorescence decreases within mixing time due to acrylamide quenching (Ando et al., 1982). At the concentrations used in this work, acrylamide did not have any effect on the activities and properties of myosin (Ando et al., 1982).

The initial fluorescence intensity of ϵADP bound to S-1 was higher in the presence than in the absence of BeF_3^- (Figure 5). By analogy with the vanadate effect (Rosenfeld & Taylor, 1984), this was most likely due to the increased ϵADP binding to S-1 in the presence of BeF_3^-. Following the addition of ADP, the instantaneous fluorescence intensity decrease was very small in the presence of BeF_3^- (4%, Table I) and much larger in its absence (20–22%) (curve x in Figure 5, Table I). Such differences are indicative of the different amounts of readily quenchable free ϵADP in equilibrium with M·ADP and M*·ADP·BeF_3^-. This observation is consistent with the results of the dialysis experiment and suggests that BeF_3^- enhances nucleotide binding to myosin.

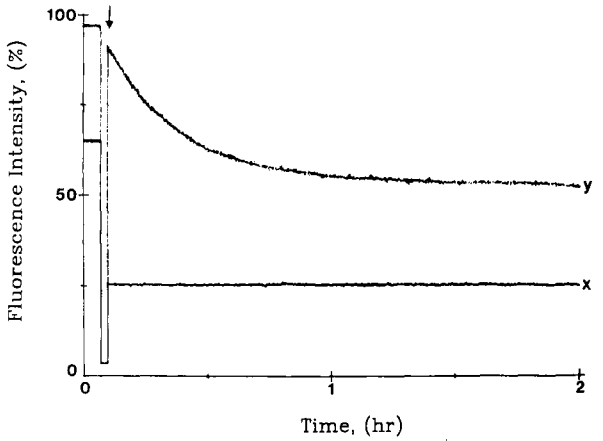

FIGURE 5: Chase of ϵADP by ADP. The release of ϵADP from S-1 in the presence and absence of BeF_3^- was examined by ADP chase. S-1 (18 μM) and ϵADP (15 μM) were preincubated for 10 min with (curve y) or without (curve x) beryllium fluoride. At the time indicated (arrow), ADP (300 μM) was added. Fluorescence intensities were measured at 410 nm in the presence of acrylamide (100 mM). The decrease in fluorescence intensity is correlated with the release of ϵADP to the quenching medium. The k_{off} rates determined for the fast and slow phases in curve y were 4.0×10^{-4} and $\sim 10^{-6}$ s^{-1}, respectively.

Table I: Fluorescence Intensities (%) of ϵADP[a]

	quencher		
experimental system	none	acrylamide (100 mM)	acrylamide (100 mM) + ADP (300 μM)
ϵADP	100	13 (±2)	
ϵADP + S-1	99 (±2)	35 (±1)	13 (±2)
ϵADP + S-1 + BeF_3^-	99 (±1)	57 (±2)	53* (±1)

[a] Fluorescence intensities of ϵADP (15 μM) were measured at 410 nm in the absence or presence of S-1 (18 μM), Be (100 μM), and NaF (5 mM). Acrylamide (100 mM) was added to quench the free ϵADP. ADP (300 μM) was used as the chase of ϵADP. Higher concentrations of ADP did not change the chase results. The fluorescence intensities were normalized to the intensity of ϵADP alone. The asterisk indicates the initial fluorescence intensity immediately after the addition of ADP.

The decay of fluorescence intensity over a 2-h chase (curve y in Figure 5) was biphasic. The rates of ϵADP release (k_{off}) in the two phases were estimated by fitting the data to two exponential expressions with the final end point fixed at the value expected for full dissociation of ϵADP. For the fast phase, the k_{off} was 4.0×10^{-4} s^{-1}, and the slow phase had a rate of ϵADP release close to 10^{-6} s^{-1}. The biphasic fluorescence decay observed in the chase experiments agrees with the biphasic reactivation of S-1 seen in the dialysis experiments. These results indicate that an additional, very slow third kinetic step, leading to a transition of M*·ADP·BeF_3^- to a virtually irreversibly inhibited complex, M'·ADP·BeF_3^-, at a rate k_3, should be included in Scheme I. Such a slow step, governed by k_3, would have a negligible, if any, effect on all kinetic and binding parameter determinations.

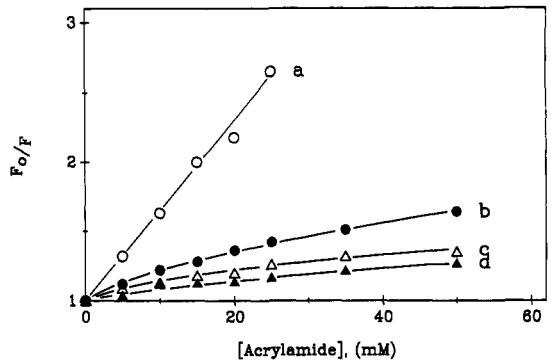

FIGURE 6: Stern–Volmer plots of acrylamide titrations for ϵADP and S-1 + ϵADP + Be. The accessibility of ϵADP to quenchers was monitored by acrylamide titrations of ϵADP (○), S-1 + ϵADP (●), S-1 + ϵADP + Be + NaF (▲), and S-1 + ϵADP + NaV_i (△). F_o/F was determined by dividing the initial fluorescence intensity (F_o) by the fluorescence intensity (F) at any given acrylamide concentration. The solvent contained 10 mM PIPES, 30 mM KCl, and 1 mM $MgCl_2$, 20 °C, pH 7.0. For ϵADP, the nucleotide concentration was 20 μM. For S-1 + ϵADP, the S-1 concentration was 25 μM, and the ϵADP concentration was 8 μM. At these concentrations of protein and nucleotide, about 70% of nucleotide was bound to S-1 (Rosenfeld & Taylor, 1984). For S-1 + ϵADP + Be + NaF, the S-1 concentration was 25 μM; ϵADP, 8 μM; Be, 100 μM; and NaF, 5 mM. For S-1 + ϵADP + NaV_i, the conditions reported by Rosenfeld and Taylor (1984) were used except that the S-1 concentration was 35 μM and the reaction mixture was passed through Penefsky (1977) column twice after dialysis to remove the free V_i.

Conformation Properties of M^*·ADP·BeF_3^-. (*A*) *Tryptophan Fluorescence.* One of the characteristic features of the M^{**}·ADP·P_i complex is the enhanced tryptophan fluorescence of myosin (Werber et al., 1972). To determine whether the complex M^*·ADP·BeF_3^- exhibits the same property, the tryptophan fluorescence of S-1 was measured in the presence of MgADP and BeF_3^-. Together, BeF_3^- and MgADP enhanced the tryptophan fluorescence of S-1 by 16% (±2%). The fluorescence increase was completed within 3–5 min after S-1 was mixed with the ligands, which corresponded to the isomerization step. The 16% increase in tryptophan fluorescence was smaller than the change observed upon ATP binding to S-1 (20 ± 2%). This small difference, although within experimental error, may reflect subtle differences between the conformations of the M^{**}·ADP·P_i and M^*·ADP·BeF_3^- complexes. As expected, ADP alone produced a much smaller change (6%) in the tryptophan fluorescence of S-1 while Be and NaF alone had no effect on the fluorescence signal.

(*B*) *Accessibility of ϵADP at the Active Site of S-1 to Collisional Quenchers.* Active-site-bound nucleotides are frequently protected from the medium. For myosin, this has been demonstrated by fluorescence quenching titration of ϵADP with acrylamide (Ando et al., 1982) in which a clear distinction could be made between the free and the bound nucleotide.

In this study, the concentrations of ϵADP and S-1 were chosen such that at least 70% of ϵADP was bound to S-1. Figure 6 shows the Stern–Volmer plots for acrylamide titrations of ϵADP bound to S-1 in the presence and absence of BeF_3^-. In the presence of S-1 and BeF_3^- (curve d), ϵADP was much more resistant to acrylamide quenching than ϵADP with S-1 alone (Figure 6, curve b). A similar conclusion was reached with respect to the effect of vanadate on the accessibility of ϵADP on S-1 to quenchers (Rosenfeld & Taylor, 1984). The titration in the presence of vanadate was reproduced here (Figure 6, curve c) to facilitate the comparison with the M^*·ADP·BeF_3^- state. The similarity between curves c and d in Figure 6 suggests that the complexes M^*·ADP·V_i and M^*·ADP·BeF_3^- may have analogous conformations.

The decrease in acrylamide quenching of ϵADP on S-1 due to the presence of beryllium fluoride not only resulted from the beryllium-induced increase in ϵADP binding to S-1 but also reflected real quenching differences between the M^*·ϵADP·BeF_3^- and M·ϵADP states. Under binding saturation conditions [derived from titrations of 10 μM S-1 in 200 mM acrylamide with ϵADP (up to 45 μM) in the presence and absence of beryllium fluoride], ϵADP in the M^*·ϵADP·BeF_3^- state was quenched by 15% less than in the M·ϵADP state (not shown).

Discussion

Inorganic phosphate analogues are a valuable tool for studying the conformation and structure of the steady-state intermediate of ATP hydrolysis by myosin, M^{**}·ADP·P_i, and its role in the force generation process. Vanadate, a well-known phosphate analogue, forms a strong and stable ternary complex with M·ADP (Goodno, 1979). Several studies compared the properties of the ternary complex M^*·ADP·V_i with those of M^{**}·ADP·P_i (Goodno, 1979; Goody et al., 1980; Wells & Bagshaw, 1985). X-ray diffraction experiments with glycerinated muscle (Goody et al., 1980) and kinetic studies with myosin (Goodno, 1979; Wells & Bagshaw, 1984) and actomyosin (Goodno & Taylor, 1982) suggested a conformational analogy between the two complexes. However, the M^*·ADP·V_i complex did not exhibit the characteristic enhanced protein fluorescence of the M^{**}·ADP·P_i state (Bagshaw & Trentham, 1974; Goodno, 1979). Furthermore, vanadate has been known to undergo extensive polymerization (Pope & Dale, 1968; Rieger, 1973) which could influence the detailed kinetic analysis of the M^*·ADP·V_i formation.

In this study, we have examined the interaction of another phosphate analogue, BeF_3^-, with myosin. The interaction of BeF_3^- with myosin has many common features with the interaction of vanadate and myosin. First, BeF_3^- is an effective inhibitor of the myosin ATPase. Yet, when added to the assay system, i.e., in the presence of ATP, BeF_3^- inhibits the ATPase activity at a very slow rate ($k_{obs} = 4.8 \times 10^{-5}$ s^{-1}). The onset of the inhibition is much faster, by approximately 2 orders of magnitude ($k_{obs} = 5.8 \times 10^{-3}$ s^{-1}), when BeF_3^- is preincubated with S-1 and MgADP. Both qualitatively and quantitatively, these observations are similar to what has been reported for the inhibition of myosin ATPase by vanadate (Goodno, 1979). The large kinetic differences between the rates of myosin inhibition in the presence of ADP and ATP show that the formation of the inhibitory complex requires the presence of MgADP at the active site. During the steady state of ATP hydrolysis, the concentration of M·ADP species is very low, decreasing at 25 °C to ≤4% of the total active-site concentration (Trentham et al., 1976). Thus, the much slower inhibition of myosin by BeF_3^- in the presence of ATP than in the presence of ADP is consistent with the suggestion that M·ADP is the main intermediate in the inhibition pathway. Certainly, BeF_3^- either does not access the active site in the presence of MgATP or does not displace P_i well enough from the main steady-state species M^{**}ADP·P_i. The same conclusion has been reached with respect to the inhibitory action of vanadate (Goodno, 1979).

The inhibition of myosin ATPase by BeF_3^- must involve at least a two-step process. A third step is required to account for the very slow transition of M^*·ADP·BeF_3^- into a virtually irreversibly inhibited complex, as detected in dialysis or long incubation chase experiments. For all other purposes, i.e., for the description of inhibition, binding, and short chase experiments, the above third step can be neglected. A single-step

inhibition mechanism can be excluded because of both the very slow apparent second-order rate constants and the nonlinear dependence of the observed rate constants on Be concentration. A simplified two-step process (eq 1), involving a rapid binding preequilibrium and a slow isomerization step between M·ADP·BeF_3^- and M*·ADP·BeF_3^-, is analogous to the inhibition mechanism proposed for vanadate (Goodno, 1979). For simplicity of presentation, it is also assumed that additional binding equilibria between myosin and ADP can be neglected in eq 1; i.e., that in the preincubated samples, M·ADP is the dominant form of myosin prior to the addition of BeF_3^-. This assumption is valid under the chosen experimental conditions of a 100-fold molar excess of ADP (300 μM) over S-1 (3 μM) and given the strong binding of MgADP to myosin (Eisenberg & Greene, 1980). We have also verified in a separate set of experiments, in which the concentration of BeF_3^- was fixed and that of ADP varied, that almost complete inhibition of myosin ATPase was obtained at ADP concentrations of 300 μM and below.

An additional description of the two-step inhibition mechanism can be derived from the examination of other parameters measured in this work. The concentration of BeF_3^- at half-maximum inhibition rate (Figure 2) provides an estimate of the equilibrium constant (K_1) of the initial complex M·ADP·BeF_3^- of 10^4 M^{-1}. The overall binding constant of BeF_3^- and M·ADP of 5×10^5 M^{-1}, determined from Figure 3, is equivalent to a good approximation to the product of the two equilibrium constants K_1 and K_2. Thus, the estimate of the equilibrium constant for the isomerization reaction is K_2 = 50. The rate constant k_{-2} of the isomerization step can be equated with the k_{off} rate of the fast phase measured in the ϵADP chase experiments (4.0×10^{-4} s^{-1}) provided, of course, that similar preincubation times are used in all measurements. The use of rate constants determined for ϵADP in the scheme involving ADP is justified by the fact that apparent rate constants of ϵADP and ADP dissociation from S-1 are indeed similar (1.0 and 1.4 s^{-1}, respectively; Rosenfeld & Taylor, 1984). Also, although the reversal of the isomerization does not involve ϵADP dissociation, the rate-limiting step in the ϵADP release is governed by k_{-2}. Thus, k_{off} provides a good estimate of k_{-2}. The forward rate constant, k_2, which has been obtained by fitting the data of Figure 2 to eq 2 and by using the above value of k_{-2}, is 1.43×10^{-2} s^{-1}, within a range of rates expected for a protein conformational change (Hammes & Schimmel, 1970). The isomerization rate k_2 can also be calculated from the equilibrium constant K_2 (=50) and the value of k_{-2} to yield $k_2 = 2.0 \times 10^{-2}$ s^{-1}. The agreement of the k_2 values derived by these two calculations also lends credence to the values of K_2 and k_{-2} obtained above. Furthermore, the k_2 determined here confirms the order of magnitude estimate made for the vanadate isomerization constant (10^{-2} s^{-1}), which could not be measured accurately because of vanadate polymerization (Goodno, 1979). It is likely that the slow isomerization rates and the accompanying conformational changes which are the basis for the locking of ADP at the myosin active site by vanadate and beryllium fluoride are similar.

The enhancement of tryptophan fluorescence following the addition of BeF_3^- to M·ADP resembles that observed for the M**·ADP·P_i complex. Yet, the small difference in the fluorescence of these complexes may reflect minor differences in their conformations. The conformation of M*·ADP·BeF_3^- seems to be analogous also to that of M*·ADP·V_i, as suggested by the similarities of their Stern–Volmer plots (Figure 6) and the kinetic constants of S-1 inhibition by beryllium fluoride and vanadate. The conformations of M*·ADP·V_i and M**·ADP·P_i differ somewhat as detected in EPR and fluorescence spectra of spin-labeled myosin filaments (Barnett & Thomas, 1987) and a fluorescent S-1 derivative (Aiguirre et al., 1986). Therefore, it is possible that the conformation of M*·ADP·BeF_3^- is slightly different from that of M**·ADP·P_i. Interestingly, when beryllium fluoride was used as a phosphate analogue to probe the mechanism of ATP hydrolysis on F-actin, the complex F·ADP·actin·BeF_3^- adopted a slightly different conformation than F·ADP·actin·P_i (Combeau & Carlier, 1988).

Even though the complex formed by BeF_3^- with M·ADP resembles the ternary complex M*·ADP·V_i, BeF_3^- is a more attractive phosphate analogue than vanadate for several reasons. First, beryllium fluoride binds to M·ADP with much higher affinity than vanadate; therefore, only low concentrations of beryllium are required for inhibition. Second, beryllium fluoride is spectroscopically silent and can be easily used in fluorescence studies. Finally, beryllium fluoride does not polymerize. These features make BeF_3^- an analogue of choice to study ATPase mechanisms.

ACKNOWLEDGMENTS

We thank Drs. E. Homsher and D. Root for helpful discussions and comments on the manuscript.

REFERENCES

Aiguirre, R., Gonsoulin, F., & Cheung, H. C. (1986) *Biochemistry 25*, 6827–6835.

Ando, T., Duke, A. J., Tonomura, Y., & Morales, A. F. (1982) *Biochem. Biophys. Res. Commun. 109*, 1–6.

Bagshaw, C. R., & Trentham, D. R. (1973) *Biochem. J. 133*, 323–328.

Bagshaw, C. R., & Trentham, D. R. (1974) *Biochem. J. 141*, 331–349.

Barnett, V. A., & Thomas, D. D. (1987) *Biochemistry 26*, 314–323.

Bigay, J., Deterre, P., Pfister, C., & Chabre, M. (1987) *EMBO J. 6*, 2907–2913.

Chase, B. P., & Kushmerick, M. J. (1991) *Muscle Motil. 2*, 247–251.

Combeau, C., & Carlier, M. F. (1988) *J. Biol. Chem. 263*, 17429–17436.

Eisenberg, E., & Greene, L. E. (1980) *Annu. Rev. Physiol. 42*, 293–309.

Fersht, A. (1977) *Enzyme Structure and Mechanism*, pp 115–117, W. H. Freeman and Co., San Francisco.

Godfrey, J. E., & Harrington, W. F. (1970) *Biochemistry 9*, 886–895.

Goodno, C. C. (1979) *Proc. Natl. Acad. Sci. U.S.A. 76*, 2620–2624.

Goodno, C. C. (1982) *Methods Enzymol. 85B*, 116–123.

Goodno, C. C., & Taylor, E. R. W. (1982) *Proc. Natl. Acad. Sci. U.S.A. 79*, 21–25.

Goody, R. S., Hofmann, W., Reedy, M. K., Magid, A., & Goodno, C. C. (1980) *J. Muscle Res. Cell Motil. 1*, 198–199.

Hammes, G. G., & Schimmel, P. R. (1970) *Enzymes (3rd Ed.) 2*, 67–114.

Issartel, J. P., Dupuis, A., Lunardi, J., & Vignais, P. V. (1991) *Biochemistry 30*, 4726–4733.

Johnson, K. A., & Taylor, E. W. (1978) *Biochemistry 17*, 3432–3442.

Kielley, W. W., & Bradley, L. B. (1956) *J. Biol. Chem. 218*, 653–659.

Lange, A. J., Arion, W. J., Burchell, A., & Burchell, B. (1986) *J. Biol. Chem. 261*, 101–107.

Lehrer, S. S., & Leavis, P. C. (1987) *Methods Enzymol. 49*, 222–236.
Maruta, S., Henry, G. D., Sykes, B. D., & Ekebe, M. (1991) *Biophys. J. 59*, 436a.
Penefsky, H. (1977) *J. Biol. Chem. 252*, 2891–2899.
Pope, M. T., & Dale, B. W. (1968) *Q. Rev. Chem. Soc. 22*, 527–548.
Rieger, P. H. (1973) *Aust. J. Chem. 26*, 1173–1181.
Robinson, J. D., Davis, R. L., & Steinberg, M. (1986) *J. Bioenerg. Biomembr. 18*, 521–531.
Rosenfeld, S. S., & Taylor, E. W. (1984) *J. Biol. Chem. 259*, 11920–11929.
Trentham, D. R., Eccleston, J. F., & Bagshaw, C. R. (1976) *Q. Rev. Biophys. 9*, 217–281.
Wagner, P. D., & Weeds, A. G. (1977) *J. Mol. Biol. 109*, 455–470.
Weeds, A. S., & Pope, B. (1977) *J. Mol. Biol. 111*, 129–157.
Wells, C., & Bagshaw, C. R. (1984) *J. Muscle Res. Cell Motil. 5*, 97–112.
Werber, M. M., Szent-Gyorgyi, A. G., & Fasman, G. D. (1972) *Biochemistry 11*, 2872–2883.
Willick, G. E., Oikawa, K., McCubbin, W. D., & Kay, C. M. (1953) *Biochem. Biophys. Res. Commun. 53*, 923–928.

Kinetic and Modeling Studies of S_3–S_3' Subsites of HIV Proteinases†

Jőzsef Tőzsér,‡,§ Irene T. Weber,‖,⊥ Alla Gustchina,‖,○ Ivo Blâha,‡,# Terry D. Copeland,‡ John M. Louis,△ and Stephen Oroszlan*,‡

Laboratory of Molecular Virology and Carcinogenesis and Macromolecular Structure Laboratory, ABL-Basic Research Program, National Cancer Institute-Frederick Cancer Research and Development Center, Frederick, Maryland 21702-1201, and Laboratory of Cellular and Developmental Biology, National Institute of Diabetes, Digestive and Kidney Diseases, National Institutes of Health, Bethesda, Maryland 20892

Received December 19, 1991; Revised Manuscript Received March 18, 1992

ABSTRACT: Kinetic analysis and modeling studies of HIV-1 and HIV-2 proteinases were carried out using the oligopeptide substrate

$$\begin{matrix} P_5 & P_4 & P_3 & P_2 & P_1 & P_1' & P_2' & P_3' & P_4' \\ \text{H-Val-Ser-Gln-Asn-Tyr*Pro-Ile-Val-Gln-NH}_2 \end{matrix}$$

and its analogs containing single amino acid substitutions in P_3–P_3' positions. The two proteinases acted similarly on the substrates except those having certain hydrophobic amino acids at P_2, P_1, P_2', and P_3' positions (Ala, Leu, Met, Phe). Various amino acids seemed to be acceptable at P_3 and P_3' positions, while the P_2 and P_2' positions seemed to be more restrictive. Polar uncharged residues resulted in relatively good binding at P_3 and P_2 positions, while at P_2' and P_3' positions they gave very high K_m values, indicating substantial differences in the respective S and S′ subsites of the enzyme. Lys prevented substrate hydrolysis at any of the P_2–P_2' positions. The large differences for subsite preference at P_2 and P_2' positions seem to be at least partially due to the different internal interactions of P_2 residue with P_1', and P_2' residue with P_1. As expected on the basis of amino acid frequency in the naturally occurring cleavage sites, hydrophobic residues at P_1 position resulted in cleavable peptides, while polar and β-branched amino acids prevented hydrolysis. On the other hand, changing the P_1' Pro to other amino acids prevented substrate hydrolysis, even if the substituted amino acid had produced a good substrate in other oligopeptides representing naturally occurring cleavage sites. The results suggest that the subsite specificity of the HIV proteinases may strongly depend on the sequence context of the substrate.

All replication competent retroviruses, including human immunodeficiency viruses, code for an aspartic proteinase [for review, see Hellen et al. (1989); Oroszlan & Luftig, 1990; Blundell et al., 1990; Debouck & Metcalf, 1990]. The major role of the retroviral proteinase (PR)[1] is the processing of the Gag and Gag–Pol polyprotein precursors. This processing is essential for the conversion of the immature noninfectious viral particles to mature infectious viruses (Crawford & Goff, 1985; Katoh et al., 1985; Kohl et al., 1988). Recent data suggest that the PR may also function in the early phase of viral infection by fragmenting the nucleocapsid protein (Roberts & Oroszlan, 1989; Roberts et al., 1991; Baboonian et al., 1991). The HIV-1 PR was also shown to be able to cleave cellular proteins like vimentin (Shoeman et al., 1990) and transcription factor NF-κB (Riviere et al., 1991). Furthermore, the cytoplasmic activation of the HIV PR of lytically

† Research sponsored in part by the National Cancer Institute, DHHS, under Contract NO1-CO-74101 with ABL.

* To whom correspondence should be addressed.
‡ Laboratory of Molecular Virology and Carcinogenesis, National Cancer Institute-Frederick Cancer Research and Development Center.
§ On leave from the Department of Biochemistry, Medical University of Debrecen, P.O. Box 6, Debrecen, Hungary.
‖ Macromolecular Structure Laboratory, National Cancer Institute-Frederick Cancer Research and Development Center.
⊥ Present address: Jefferson Cancer Institute, Thomas Jefferson University, 233 South 10th Street, Philadelphia, PA 19107.
○ On leave from the V. A. Engelhardt Institute of Molecular Biology, Academy of Sciences of the USSR, Moscow, USSR.
Present address: Czechoslovak Academy of Science, Institute of Organic Chemistry and Biochemistry, Flemingovo namesti 2, 16610 Prague, Czechoslovakia.
△ Laboratory of Cellular and Developmental Biology, National Institute of Diabetes, Digestive and Kidney Diseases, National Institutes of Health.

[1] Abbreviations: PR, retroviral proteinase; HIV, human immunodeficiency virus; SDS, sodium dodecyl sulfate, RP-HPLC, reversed-phase high-performance liquid chromatography; TFA, trifluoroacetic acid; FAB, fast atom bombardment.

0006-2960/92/0431-4793$03.00/0